Experiments on Hidden Substances Identification with Neutron Probing via Associated Particle Detection

V.M.Bystritsky, A.I.Ivanov, A.P.Kobzev, V.V.Mialkovsky, V.A.Nikitin, M.G.Sapozhnikov, V.M.Slepnev, N.V.Vlasov.

Joint Institute for Nuclear Research, Dubna, Russia.

Abstract

The paper presents description and experimental results on the search for hidden drugs and explosives substances. The approach is based on the irradiation of the hidden substance with a probing neutron beam generated in the $d + t \rightarrow \alpha + n(14.1\ MeV)$ reaction, using Van de Graaf electrostatic accelerator for producing DC deuteron beam. Detection of α particle in coincidence with γ generated in the non elastic scattering of the fast neutrons on the elements C, N, O, that are specific for drugs and explosives, provides a signature for their presence. The main parameters of the experimental setup, description of experiments and analysis of the results are given. Experiments on detection of pure chemical elements carbon, nitrogen and oxygen (water), and composite substances alcohol, carbomid and ammonium demonstrated that the relative C, N, O concentrations in composite materials could be measured with an error of $\sim$10%. It proves potential of the present approach for non-contact identification of the chemical composition of hidden and suspicious substances, including drugs and explosives.

The work was carried out at the Joint Institute for Nuclear Research, Dubna, Russia.

1 Introduction

The Associated Particle Imaging (API) is a technique which provides a three-dimensional location and chemical composition of hidden objects such as mines, explosives or drugs. The investigations of the API method were carried out in Los Alamos National laboratory [1], Argonne National Laboratory [2], Bechtel Nevada Special Technologies Laboratory [3] as well as in other laboratories (see, e.g., [4], [5]). This report describes the API system developed in the Joint Institute for Nuclear Research (JINR) and provides the results of the first experiments.

The API technique is based on the use of fast monochromatic neutrons with energy of 14.1 MeV produced by accelerating deuterium ions into tritium target in the binary reaction $d + t \rightarrow^4 He + n$. The α-particles with energy of 3.5 MeV flight back-to-back with the neutrons. By detecting the *spatial position* of the α particle the direction of the corresponding neutron is determined. These "tagged" neutrons interact with the object under interrogation and can produce γ-radiation with energy spectra which are unique for each chemical element presented in the object. By detecting the *time*

difference between arrival the α particle and the γ quanta in the corresponding detectors the distance traveled by the neutron before it scattered in the nuclei in the interrogated object is determined. It gives possibility to connect a region in the interrogated object with gamma-spectrum which irradiates just from this particular place. Therefore this method differs from thermal neutrons technique [6] or pulsed neutrons analysis [7] by providing three-dimensional image of the investigated object with low background from the neighboring regions. It significantly facilitates the identification of the chemical composition of the interrogated objects.

The purpose of our first experiments is to investigate the advantages of the API method for decreasing the background radiation in comparison with the approaches when only inclusive γ spectra are measured. The different detector shielding conditions and the object screening are tested. We have investigated also different modifications of α detector to improve the time resolution of the $\alpha - \gamma$ registration system and to increase the intensity of the neutron flux. The Monte Carlo simulations of the γ detector response is carried out for the better understanding of the detectors performance.

The created API system provides drastic decreasing of the background radiation which allows to identify different hidden substances even under conditions of heavy shielding.

2 Setup description

2.1 Accelerator and target

The scheme of the experimental setup is shown in Fig.1. The apparatus is installed at the deuteron beam of the electrostatic Van de Graaf accelerator of the Laboratory of Neutron Physics of JINR. The molecular D_2^+ beam with the energy of 400 keV per deuteron is used. The beam intensity is 0.5 μA. The target is titanium tritid - TiT_2. It is landed on stainless steel carrier which is placed at the 45^0 angle to the beam axis. The tritium surface thickness is $\sim 10^{19}$ $atom/cm^2$. The total activity of tritium is 1.7 Cu. The target and the beam control system are placed in the vacuum chamber (see Fig. 1). The beam diameter at the target is 3 mm. The neutron flux generated in $d + t$-reaction is $\sim 10^7$ s^{-1} in 4π solid angle.

2.2 Alpha detector

The α-particles are detected by the scintillator counter 3 (Fig. 1). We investigated two types of scintillators : ZnS(Ag) with light decay time τ=250 ns and plastic scintillator with τ=2.5 ns. The diameter of the both scintillators is 1 cm, they set at 7.5 cm from the target and comprises 0.011 str solid angle. The scintillator is protected from deuterons scattered in the target by 7 μm aluminum foil. The typical α-particle counting rate is $\sim 10^4$ s^{-1}. The amplitude spectra of the α- particles are presented in Fig. 2. To avoid contribution from the PMT noise and pile up events we apply the cut on the α particle amplitude shown by dashed lines in Fig. 2. The events within this interval are used for the further analysis. The ZnS scintillator produces wider right tail in amplitude spectrum in comparison with the plastic one. It is due

to pile up events. This means the plastic scintillator can be used at higher counting rate. Besides that it is necessary to stress that the use of plastic scintillator leads to appreciable background reduction.

2.3 γ-detector

We use NaI(Tl) as a gamma detector. The crystal diameter and thickness are 20 cm x 20 cm. The detector is placed at distance 45 cm from the interrogated object. Its energy calibration and resolution measurement are performed with the standard gamma sources ^{60}Co (E_γ=1.17, 1.33, 2.5 MeV) and Pu-Be (E_γ=4,43 MeV. The relative energy resolution $\delta = \sigma/E_\gamma$ at E_γ=1.33 MeV is 10% and depends on energy as $\delta \sim \sqrt{1/E_\gamma}$.

2.4 Tagged neutron beam

The center of mass of the d+t system in the binary reaction d+$t \rightarrow \alpha$+n moves in laboratory system along the X-axis (see Fig.1). It slightly destroys the back-to-back correspondence between the α and neutron trajectories. A movable scintillation counter of 4 x 4 x 0.5 cm^3 dimensions is used to measure the space distribution of the tagged neutron beam. It was found that the beam axis is deviated from the normal to the accelerator beam line on angle $\sim 7^o$. This value is in agreement with the expected one from the kinematics of the reaction. The opening angle of the neutron beam is 6.7^o. The distance between the accelerator target and the interrogated object is 85 cm. The beam width at the object position is $\sim$ 12 cm and $\sim$ 8 cm along X and Y axis, respectively (see Fig. 1).

2.5 Electronics

The data acquisition system is in Camac. The PMT's signals from α and γ detectors go to the constant fraction discriminators and to the time shapers and further to the coincidence block together with busy signal from the controller. The controller is equipped with the processor. The coincidence block generates signal of interruption for processor and strob for ADC. The signals from PMT pass through amplifiers and input to ADC resulting in amplitude spectra. To perform the time measurement the α-detector signal passes the shaper and inputs to TDC's start and γ-detector signal goes to TDC's stop. The selection of the $\alpha - \gamma$ coincidences is performed within 100 ns gate. The data readout from the converters and the data acquisition control is performed by the crate controller with build-in PC. The information stores on build-in hard disk and transfers via local net.

2.6 Apparatus time resolution

The time resolution of the $\alpha - \gamma$ system is determined in the experiments with tagged neutron beam irradiated of 12 cm graphite cube. With plastic scintillator as the α detector the time resolution is $\Gamma(FWHM) = 3.8\ ns$. In case of ZnS scintillator

the time resolution is $\Gamma = 6.0\ ns$. These values include neutron time of flight through the graphite cube which is $\Delta\tau \approx 2\ ns$.

The time properties of the α and γ detectors electronics is tested using the $\gamma - \gamma$ coincidences of two small (4 x 4 x 0.5 cm^3) plastic counters irradiated with ^{60}Co source. The distribution of the time intervals $\tau = t_{\gamma,1} - t_{\gamma,2}$ shows clear coincidence peak with $\Gamma = 2\ ns$.

One should stress here that the apparatus time resolution is the most important parameter determining background suppression and maximum possible rate of the data collection.

3 Results

3.1 Investigation of the pure substances

We start with the irradiation of the graphite, water and liquid nitrogen samples to obtain typical γ spectra of C, O and N, respectively.

The graphite sample is a cube of 12 cm with the mass 2.3 kg. In Fig.3a the time-of-flight spectrum is shown. The start is given by an α particle and the stop is by the γ signal. If γ signal is absent then compulsory stop signal generated in 100 ns after the α signal.

One can see clear two-peak structure in the time spectrum. The first peak corresponds to detection of prompt γ, produced in reaction $A(n, n'\gamma)A$. The second peak caused by the neutrons scattered in the sample and reaching the NaI(Tl) detector later. The delay time is about 8-9 ns. It corresponds to the time which is needed for a neutron with the velocity around 5 cm/ns to pass the distance 45 cm between the sample and the detector. The clear separation of two peaks significantly improves the subtraction of the background. The flat part of the spectrum in Fig.3a corresponds to the random $\alpha - \gamma$ coincidences. One should notice that the plastic used in the α-detector gives higher ratio R signal-to-background and, as consequence, better separation of the two peaks in the time spectrum. For plastic the ratio signal-to-background is $R \approx 12$ and for ZnS $R \approx 4$.

The Fig.3b shows the γ energy spectrum (with plastic α detector) without any time selection. Fig. 3c shows the same spectrum with the time selection. The time gate is indicated on Fig.3a ($\Delta\tau$=2 ns). One can see dramatic background reduction and carbon 4.43 MeV line becomes very clear.

The data on Fig. 4 demonstrate different origin of the two peaks in the time distribution for carbon object. Fig. 4a shows the time gate positions. Fig. 4b presents γ energy spectrum of the events selected in time interval Δt_1. The shaded area is background distribution measured without the graphite cube. Fig. 4c shows the energy spectrum after subtraction the background. The carbon 4.43 MeV γ-line is clearly dominated in this spectra. The first escape line shifted to the left by 0.51 MeV is also well resolved. The left tail in Fig.4c is due to the γ-ray Compton effect modified by the electronics threshold and the detector efficiency. Fig. 4d,e present γ energy spectra of the events selected in time interval Δt_2. These spectra are smooth

as it is expected if the second peak in the time distribution is generated by the delayed neutrons rescattered in the graphite cube.

The Fig. 5 summarized the data taken with graphite, liquid nitrogen (1.5 liters) and water (1.5 liters). Left column a) shows the energy spectra of γ quanta obtained without time selection. Shadowed histograms corresponds to the measurements of the background, performed without the investigated objects. The middle column b) shows the energy spectra with time selection. We choose 2 nc interval in the first peak of time distribution as described above. The right column c) corresponds to the energy spectra with time selection and subtraction of the background.

Comparing plots of 5a) and 5b) one could see how the time selection drastically reduces the background. The ratio between open and shadowed regions increases significantly for the time selection plots of 5b). After time selection it is possible to see typical peaks corresponding to some well known γ-transitions. It is especially remarkable in case of oxygen and nitrogen, where without time selection the energy spectrum of Fig. 5a) looks absolutely monotonous. Whereas after the time selection the most intensive lines in ^{14}N at 5.1 MeV and ^{16}O at 6.13 MeV are looking clearly. The corresponding escape lines are also observable.

We checked the effect of the container walls on the γ-spectra shape. The graphite cube was exposed in two steel containers with wall thickness of 6 and 12 mm. In Fig. 6a) the corresponding time distributions are shown. One could see that the additional shielding is smearing the first peak in the time distribution, as it expected. However the γ spectra shown in Fig. 6b) after the same procedure of time selection are practically unchanged. One may conclude that the effect of the wall thickness is not crucial.

3.2 Monte Carlo simulation of the γ-detector response.

Monte Carlo simulation of NaI(Tl) detector response in coincidence with α-detector has been done using the GEANT3 package (version 3.21) [8]. The irradiated object is carbon. Photons, electrons and positrons are followed down to energies of 10 keV. To handle the low-energy neutrons in the range $10^{-5}\ eV \leq E_n \leq 20\ MeV$ GEANT-MICAP interface is used. To obtain a correct NaI(Tl) response to γ the following energy resolution parametrization was applied in the simulations: $\delta = \sigma/E_{depos} = \sqrt{A/E_{depos}}$, where E_{depos} is energy deposition in NaI(Tl) detector; A = 0.0425 MeV - parameter resulting from the fit of former formula to the data from calibration runs with standard gamma sources Co^{60} and Pu-Be.

The simulated time distribution is shown in Fig. 7a. It is in qualitative agreement with the experimental spectra shown for comparison in Fig. 7b. The second peak in MC spectrum has a smaller intensity comparing with the experimental one. This may be due to not adequate account of the neutron interactions with NaI in the GEANT code. But this slight disagreement in the region of the second peak must not effect our results based on analysis of the first peak. This is clear from Fig. 7b, since overlapping of two areas is negligible - less than 2%. Fig. 7c demonstrates good agreement of experimental and MC energy spectra with the time selection in the interval Δt_1 . In summary we can infer from these data that we have rather good understanding of the

apparatus performance and could use the Monte Carlo simulation for the optimization of the detector characteristics.

3.3 Investigation of the composite substances

The composite substances alcohol (C_2H_5OH), carbomid (CH_4ON_2), and ammonium (NH_4NO_3) was studied. The corresponding γ energy spectra are shown in Fig. 8. Left column a) shows the energy spectra of γ quanta obtained without time selection. Shadowed histograms corresponds to the measurements of the background, performed without the investigated objects. The middle column b) shows the energy spectra with time selection. We choose 2 nc interval in the first peak of time distribution as described above. The right column c) corresponds to the energy spectra with time selection and subtraction of the background.

For the composite substances the effect of the time selection is even more significant. The energy spectra without time selection 8a) looks absolutely smooth, without any characteristic gamma-lines. However the time selection provides strong suppression of the background. In result, we indeed obtained a sequence of gamma-peaks which is typical for each concrete substance.

Especially interesting is comparison of the carbomid spectrum with the ammonium one. The carbomid (CH_4ON_2) spectrum is dominated by the peak of carbon at 4.43 MeV whereas in the ammonium (NH_4NO_3) spectrum the peaks of oxygen and nitrogen are clearly seen.

One may conclude that the time selection really drastically suppress the background and provides the best conditions for the identification of the composite substances.

3.4 Evaluation of the chemical formula.

We calculate the chemical composition of the two component object using the following equation:

$$\frac{N_1}{N_2} = \frac{n_1 \cdot \sigma_1(E_1) \cdot f(E_1)}{n_2 \cdot \sigma_2(E_2) \cdot f(E_2)} \tag{2}$$

Here $N_1,\ N_2$ are the counting rates observed in amplitude spectrum within the γ peaks "l" and "2". $n_1,\ n_2$ are unknown atom concentrations of the element "1" and "2" in the chemical compound. σ_i are corresponding cross sections of the $(n\gamma)$ reaction, E_i are energies corresponding to the γ peaks, f is the efficiency of the γ detection by means of NaI(Tl) counter. Applying this formula to the alcohol data (C_2H_5OH) we got the carbon to oxygen concentration ratio $R(C/O)$ as $R(C/O) = 1.95 \pm 0.2$. The identification of the three component substances requires more elaborate date analysis which we plan to perform in the nearest future.

4 Conclusion

From the experience gained and studies made in the course of the present work we drew the following conclusions.

1. Our results show that developed experimental technique is capable to identify pure and some composite substances hidden in the containers.

2. The use of α-detector based on the plastic scintillator (instead of usually applied inorganic ZnS(Ag) scintillator) makes possible:

a) to get better $\alpha - \gamma$ time resolution: $\Gamma(FWHM) = 3.8\ ns$.

b) to increase signal-to-background ratio R in $\alpha - \gamma$-coincidence: $R = 12$ for plastic and $R = 4$ for ZnS;

c) to increase upper limit of the neutron source intensity up to $10^8\ n/s$ and keep reasonably good parameters $\alpha - \gamma$ detecting system - the energy and time resolution, the rate of pile up events does not exceeds 10%.

3. The optimization of the γ-detector position relative to the object and making its reasonable radiation shielding makes possible clear time separation of prompt γ and background (mainly neutron) events.

4. There is good agreement between the experimental data and its Monte Carlo simulation. This correct understanding of the process of the neutron interaction with the interrogated object gives possibilities for the correct identification of the chemical elements C, N and O concentrations, which are basic constituents of the illicit substances.

In order to determine chemical formula of composite substances it is require to work out a method of description of complicated amplitude spectra obtained by means of NaI(Tl) detectors. The further improvement of the apparatus energy and time resolution is also the goal of our future efforts.

5 Acknowledgment

It is a pleasure for us to thank Prof. V.G.Kadyshevsky for his important advises at the beginning of this work in Dubna.

We would like to thanks Prof. B.Maglich and Prof. V.Bystritskii for their constant interest and many useful discussions. We are grateful to Yu.K.Nedachin, the director of the Scientific Production Centre "Aspect" and Russia State Customs Committee for providing the essential financial support.

It is a pleasure for us to thanks I.A.Chepurchenko for providing a stable operation of the Van-de-Graaf accelerator and V.A.Budilov for electronics and counters preparation.

References

[1] L.I.Ussery et al. Los Alamos Nat. Lab report LA12847-MS (October 1994).

[2] E.Rhodes at al., SPIE, v. 2092, p. 288 (1993) E.Rodes et al., APSTING: Associated Particle Sealed Tube Neutron Generator Studies for Arms Control. ANL report ANL/ACTV-95/1 (1994)

[3] J.P.Hurley et al. Current status of the Assosiated Particle Imaging System at STL. EGG-10617-3008 (January 1992).

[4] B.C.Maglich et al., Atometry. Hienergy Report, Hien 98-111, Sept. (1998).

[5] G.Vesti et al., Nucl.Instr.Meth., A422 (1999) 918.
G.Vesti et al., preprint DFPD 99/NP/43.

[6] P.M.Shea et al. Nucl. Instr. Meth., A299, p.444, (1990) A.Fainberg. Science, v. 255, p. 1531, (1992).

[7] D.R.Brown et al., Nucl. Instr. Meth., A353, p. 684, (1994).

[8] GEANT:Detector description and simulation tool, CERN Program Library W5013, Geneve, 1994.

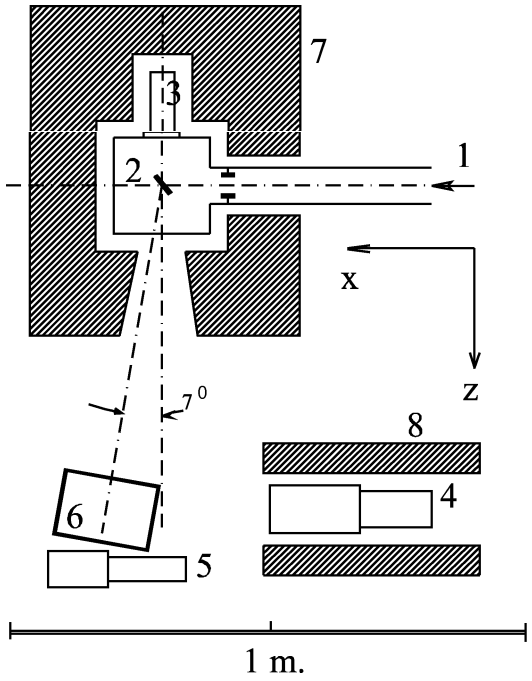

Fig. 1. Setup schematic layout.
1. Deuteron beam line of the accelerator.
2. TiT_2 target. 3. Alpha detector.
4. NaI(Tl) detector. 5. Neutron detector.
6. Interrogated object. 7. Radiation shield, $CH_2 + B$. 8. Radiation shield, Pb.

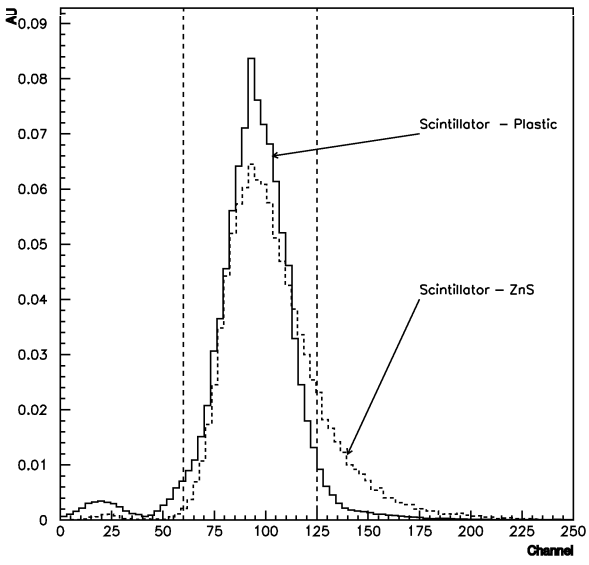

Fig. 2. Alpha particle amplitude spectrum. The comparison of the two scintillators response is presented.

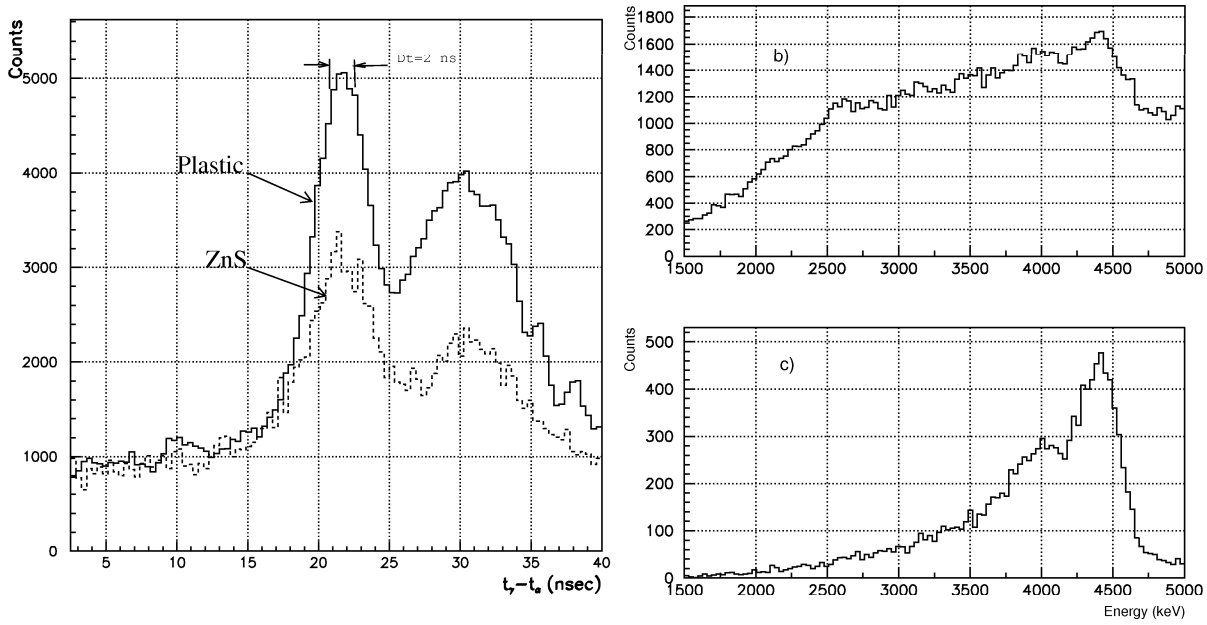

Fig.3. a) The carbon object. $\alpha-\gamma$ coincidence time distribution. The performance of two scintillators in the α-detector is shown, indicating some advantage of plastic versus ZnS(Ag).

b) The γ energy spectrum without time selection (plastic α detector).

c)The γ energy spectrum with time selection. The gate is indicated in Fig.3a.

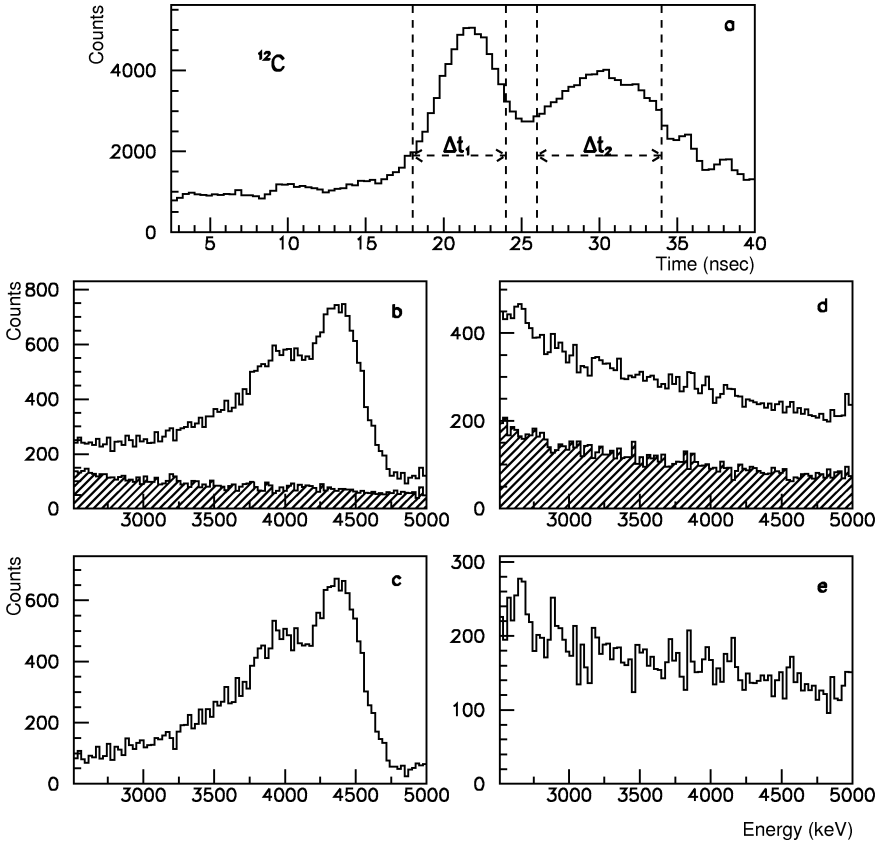

Fig. 4. The time and energy spectra taken with carbon object. a)The time distribution. The time gates are shown for further data analysis. b) γ energy spectrum for events selected in Δt_1 gate. Shaded area is the background. c) - The same as in a) after background subtraction. d) and e) The same as in d) and c) but for event selected in Δt_2 time interval.

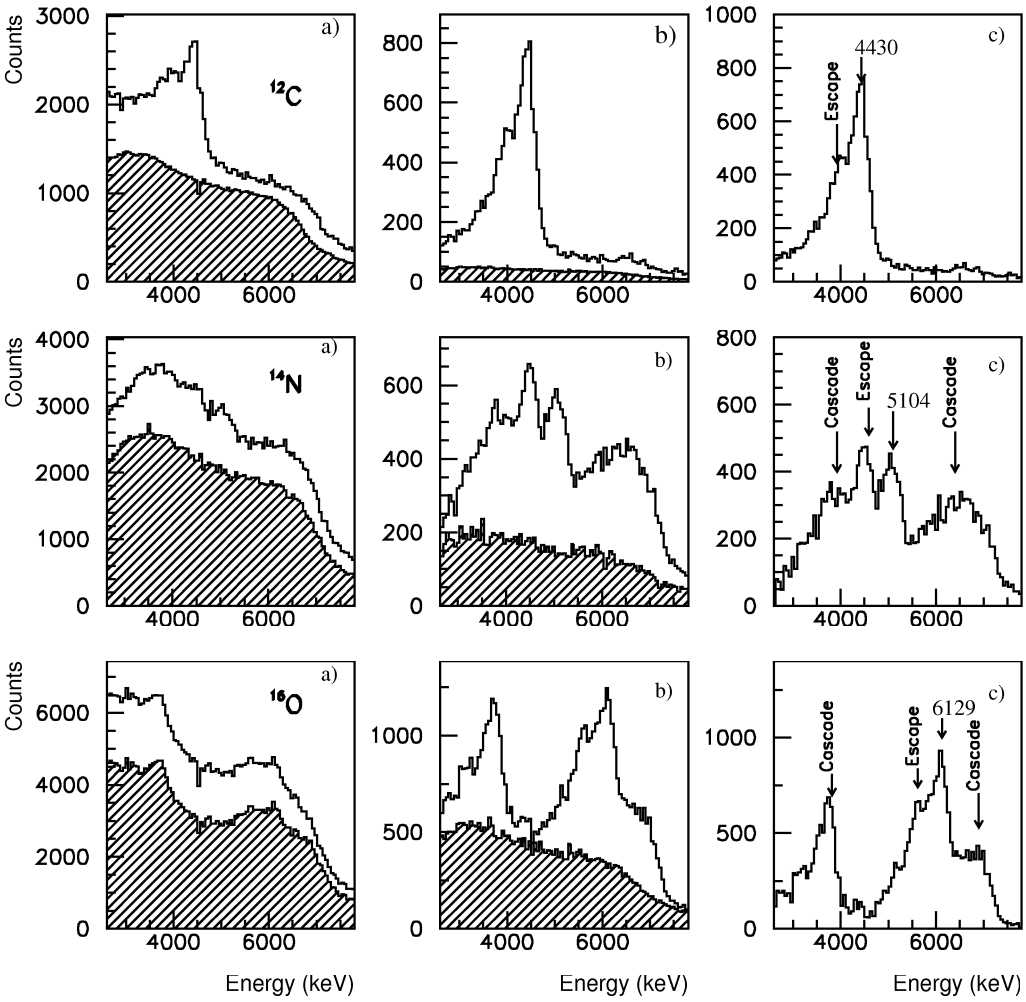

Fig. 5. The γ energy spectra of the pure substances. a) - Without time selection criterion. b) - With time selection criterion. c) - With time selection criterion and background subtraction.

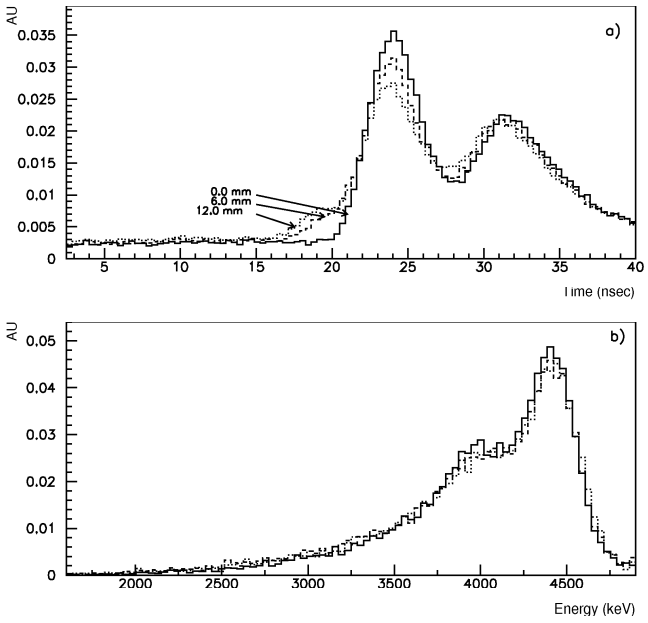

Fig. 6. The object is graphite placed in steel containers with wall thickness 6 and 12 mm. The effect of walls on γ time and energy spectra is demonstrated. a) - time distribution, b) - energy spectra.

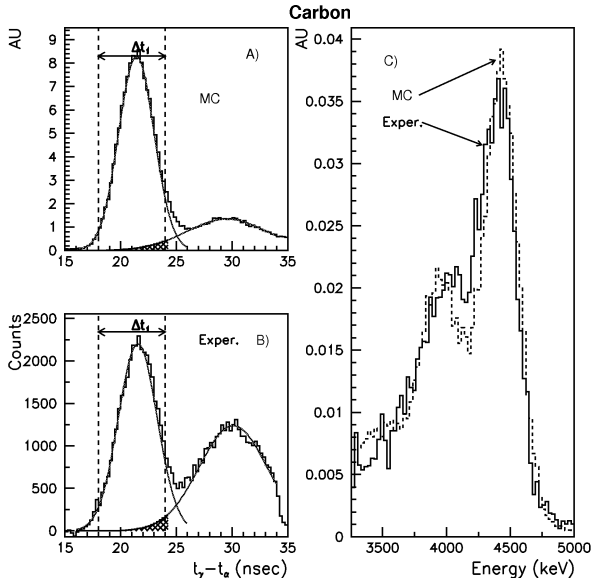

Fig. 7. Comparisons of the Monte Carlo simulated time distribution a) with the experimental spectrum b). The Monte Carlo and the experimental energy spectra are compared in c).

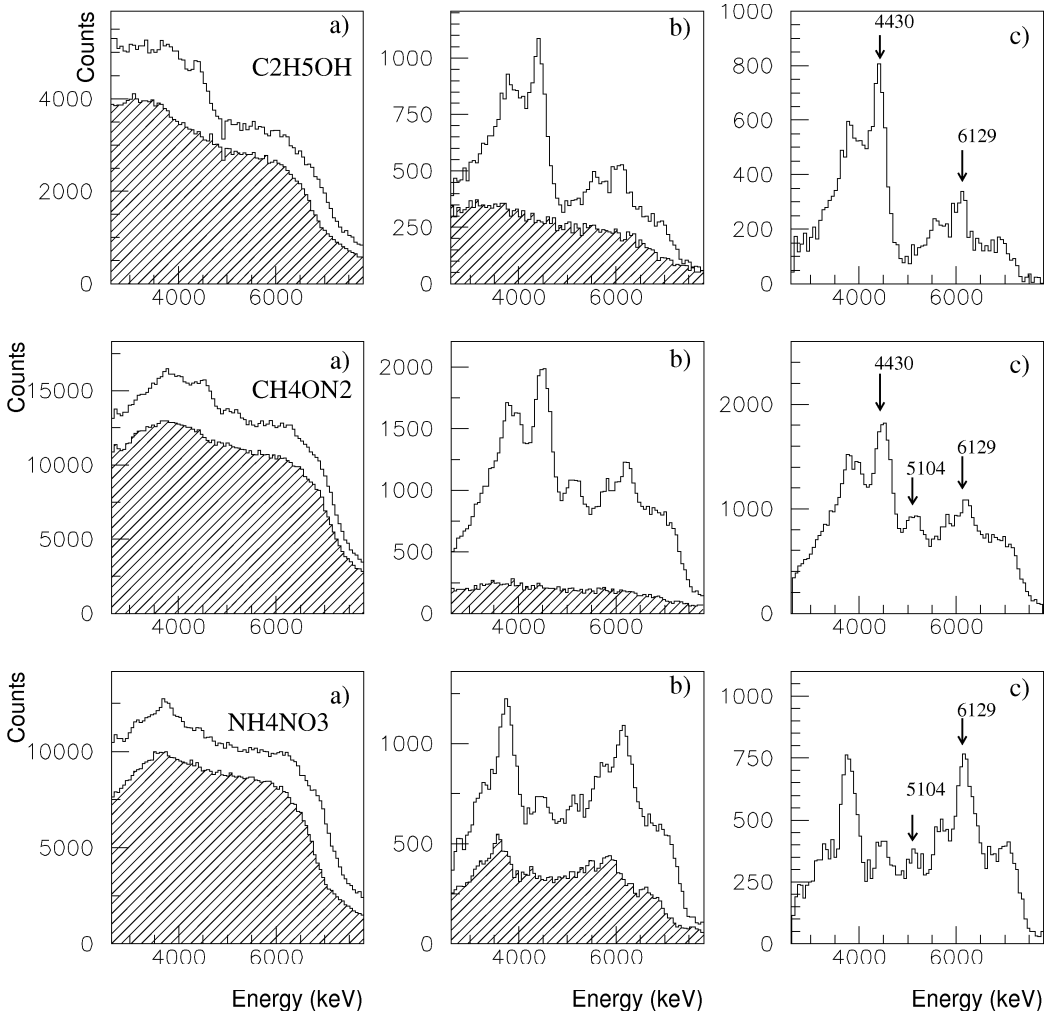

Fig. 8. The energy γ-spectra of the composite substances. a) - Without time selection criterion. b) - With time selection criterion. c) - With time selection criterion and after background subtraction.